Science Advances Today

Sci. Adv. Today 2 (2016) 25242

Fiber Bragg gratings embedded in 3D printed prototypes

Daniel Homa*, Cary Hill, Adam Floyd, and Gary Pickrell

Virginia Polytechnic Institute and State University, 213 Holden Hall, Blacksburg, VA, 24061, USA

*Author for correspondence: Daniel Homa, email: dan24@vt.edu

Received 06 Jul 2016, Accepted 29 Aug 2016, Published Online 29 Aug 2016

In this study, we incorporated fiber optic sensors in 3D printed prototype parts. Fiber optic Bragg gratings embedded in polylactic acid were configured to measure strain and/or temperature. Residual non-uniform stresses in the 3D printed parts induced spectral distortions in the FBGs such as peak broadening and wavelength hopping. Local isolation of the FBG in a used quartz capillary tube minimized the spectral distortion and peak wavelengths were readily identifiable with commercial interrogation software. The seamless integration of robust optical fiber sensing techniques and additive manufacturing processes is readily feasible, via proper implementation and interrogation schemes, for a wide array applications to include structural health monitoring and real-time component diagnostics.

1. INTRODUCTION

Additive manufacturing, or more commonly known as "3D printing", technologies have been gaining popularity in research laboratories, manufacturing plants, and in the homes of backyard inventors, alike. Although the first 3D printer was made by Charles Hull over 30 years ago, these techniques have just recently experienced rapid mainstream adoption [1]. Although, at this time, 3D printing has found a niche as a tool for rapid prototyping, the breadth of potential uses is almost limitless to include medical applications, aerospace component manufacturing and device fabrication [2-5].

The additive manufacturing process also provides a unique means for the fabrication of smart materials for real-time structural health monitoring [6]. Sensors can be incorporated into the component during the fabrication process to allow for assessment of component integrity via temperature and strain measurements [7, 8]. Specifically, fiber optic sensors are well suited for a smooth integration with 3D printing technologies because of their well-known advantages such as their light weight, small size, and immunity to electromagnetic interference [9, 10]. Fiber optic sensing technologies can be readily configured for single point, distributed, and/or fully distributed measurements with sensors such as fiber Bragg gratings (FBGs), Fabry Perot interferometers (FP), and back scatter interrogation techniques. Furthermore, fiber optic sensors have been proven reliable for an extremely wide array of applications and have emerged from the development plateau to commercialization [11].

Fiber optic sensors are often integrated with materials to measure specific properties. For example, sensors such as FBGs and FPs have been bonded to magnetostrictive materials to sense magnetic fields and have recently been exploited to evaluate the performance characteristics of the epoxies, themselves, used to adhere the sensors to the material of interest [12-14]. The intense interest in smart materials and structure health monitoring has inspired the incorporation of fiber sensors in composite structures to monitor parameters such as strain and temperature [15-17]. Recently, this basic approach has extended to the integration of fiber Bragg grating technologies and additive manufacturing processes to evaluate the residual strain and temperature of the prototype parts during and after fabrication process [18-22]. Although intriguing, discussions of the FBG spectral characteristics and optimization are limited, and necessary to demonstrate the viability of this basic approach.

Generally, a FBG is a periodic refractive index change etched into an optical fiber via exposure to selected UV radiation. The effective refractive index profile, $n_{eff}(z)$ as a function of position along the FBG is described as the following,

$$n_{eff}(z) = n_0 + \partial n(z)\left\{h + \cos\left[\frac{2\pi}{\Lambda(z)} z\right]\right\} \quad (1)$$

where z is the distance along the fiber longitudinal axis, n_0 is the initial effective refractive index of the fiber, $\delta n(z)$ is the envelope of the effective refractive index change, h is the background component of the effective refractive index change, and $\Lambda(z)$ is the grating period [22, 23]. Fiber Bragg gratings have been successfully deployed as sensors because their properties of the grating are a very sensitive to a host of external perturbations. For example, a shift in the Bragg wavelength, $\Delta\lambda_B/\lambda_B$ can be readily correlated to an uniform applied temperature or strain per the following,

$$\Delta\lambda_B/\lambda_B = (1 - p_e)\varepsilon + (\alpha_\Lambda + \alpha_n)\Delta T \quad (2)$$

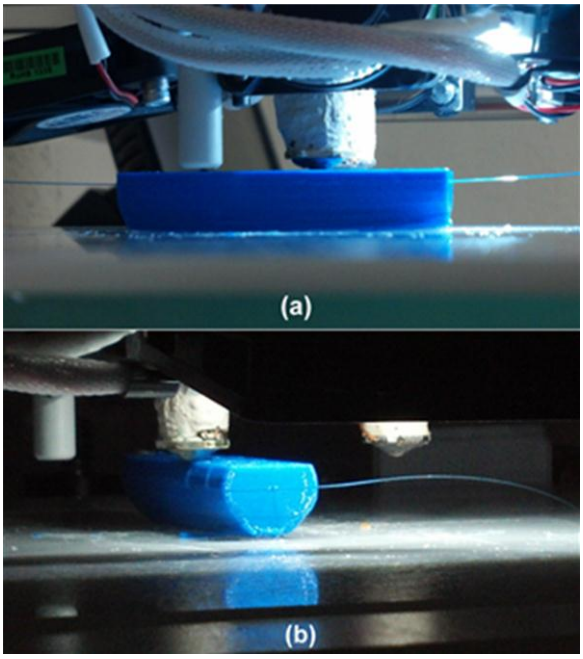

Figure 1. Fiber optic sensor embedment in part during the 3D printing process; (a) side and (b) end face view.

where p_e is the strain optic coefficient, ε is the applied strain, α_Λ is the thermal expansion coefficient of the fiber, α_n is the thermo-optic coefficient, and ΔT is the temperature change [24]. Although cross sensitivity of the FBG to these perturbations is very relevant, we have attempted to minimize these effects and in our study, and neglected any temperature effects and evaluated the response of the FBGs to residual and applied strain.

Unfortunately, embedded FBGs intimately interact with the host material and experience a non-uniform strain that often results in very local strain fields within the FBG [25-27]. This strain variation can induce coupling between the cladding and core modes resulting in spectral distortion, wavelength hopping, and peak broadening [28-30]. Subsequently, the automated software cannot accurately track the Bragg wavelength, which often manifests in significant or catastrophic measurement errors. Thus, significant efforts have been dedicated to understand the observed FBG spectral phenomena and deconvolute the secondary gratings that form within the primary grating [30-33]. Successful development of accurate FBG spectral models may allow for more detailed strain (and temperature) profile within the host material.

The majority of applications, though, do not require the high spatial resolution potentially achieved with the analysis of intracore gratings. Thus, the FBG can be encased in a fused quartz capillary tube to "locally" isolate it from the host material [34]. In turn, the strain measurement resolution will be dictated by the distance between the points at which the fiber is bonded to the host point, which is typically on the order of 5-10 mm. Although the resolution of the measurement is reduced, the improvement in the FBG spectral integrity dramatically improves the interrogation approach

The objective of this work is to demonstrate the feasibility and challenges of fiber optic sensing in 3D printing technologies. In this study, we successfully embedded fiber Bragg gratings in polylactic acid (PLA) prototypes fabricated with a commercially available 3D printer. The performance and spectral characteristics of the FBGs were evaluated after embedment and upon tensile loading. Specifically, this work evaluates the embedded response of printed part density on non-isolated (no protective sheath) FBGs, the embedded frequency response of non-isolated FBGs, and the embedded frequency response of isolated FBGs. The spectral integrity preserved in an FBG encased in a fused quartz capillary allowed for accurate peak wavelength tracking and strain measurements.

2. MATERIALS AND METHODS

2.1. Materials

The plastic parts were fabricated with a 3D Systems CubeX™ purchased from Technology Education Concepts, Inc. The plastic filament, polylactic acid (PLA), was packaged in a plastic cartridge and acquired from 3D Systems. Bare fiber Bragg gratings (FBGs) inscribed in SMF28 type used in this study were acquired from Oeland. The round clear quartz capillary tubes were acquired from Vitrocom and maintained an inner diameter of 200 µm and outer diameter of 330 µm.

2.2. Component Fabrication

The "host" parts were fabricated via plastic jet printing. First, the prototype design was converted into a print file utilizing the software provided by 3D Systems. The temperature and x-y position of the jet was dictated by these design parameters, as well as the z position of the print plate. Generally, the filament was continuously fed into the jet and melt-extruded, at temperature of approximately 240°C, onto the print plate. The movement of the ink jet was synchronized with the position of the non-heated print bed, which lowered incrementally after each layer was deposited to "build up" the part. The optical fiber sensor was manually set in the part in-situ with the printing process, under slight tension to restrict movement, as shown in Figure 1 for a cylindrical part. The peak positions and fiber Bragg grating spectrums were continuously monitored with a Micron Optics SMF125 optical interrogator and Enlight software.

The printed prototypes were type 3 ASTM 638 parts typically used for tensile testing of polymers. The prototype specific to this study maintained an overall length of 148.10 mm, a thickness of 8.38 mm and width of 17.22 mm, and a layer thickness of 0.25 mm. Parts were printed with hollow, medium and thick densities without a support or raft material to evaluate the effects on the FBG spectral quality.

2.3. Performance Testing

The performance of the 3D printed prototypes and embedded FBGs was evaluated via traditional mechanical tests. A 95 Series model from Com-Ten Industries was used for all the tensile tests, and the FBG properties were monitored continuously with the Micron Optics SMF128 optical interrogator and the companion Enlight software. An increasing load was applied to the ASTM component (gauge length of 76.7 mm) and stopped prior to catastrophic failure and slowly decreased to remove the slightly elongated specimen.

3. RESULTS AND DISCUSSION

3.1. Embedded FBGs

Spectral distortions were observed for the fiber Bragg gratings that were incorporated in the parts during the 3D printing process, as shown in Figure 2. Non-uniform residual stresses inherent to the additive manufacturing process can alter the FBG properties such as the spectral shape and polarization state, as well as induce wavelength hopping and microbend losses. Although this phenomenon has been noted in composite structures and epoxy bonding, and exploited in acoustically induced grating structures, not much has been discussed with respect to materials fabricated via 3D printing [30, 32, 35].

The fiber Bragg grating embedded in a 3D printed part with a medium density shift, broadened and shifted to lower wavelengths, as shown in Figure 2 (a). As shown in Figure 2 (b), FBG peak splitting was observed in the test specimen fabricated with a thick density. The spacing between successive layers oriented perpendicular to the axis of the FBG created the necessary periodic refractive index change within the grating structure to cause the single FBG to "split" into two FBGs.

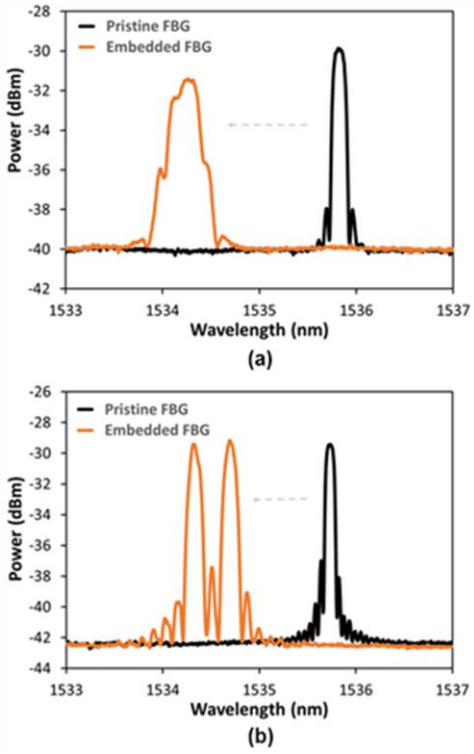

Figure 2. Spectral distortion of fiber Bragg gratings upon embedment in parts printed with a (a) "medium" and (b) "thick" build.

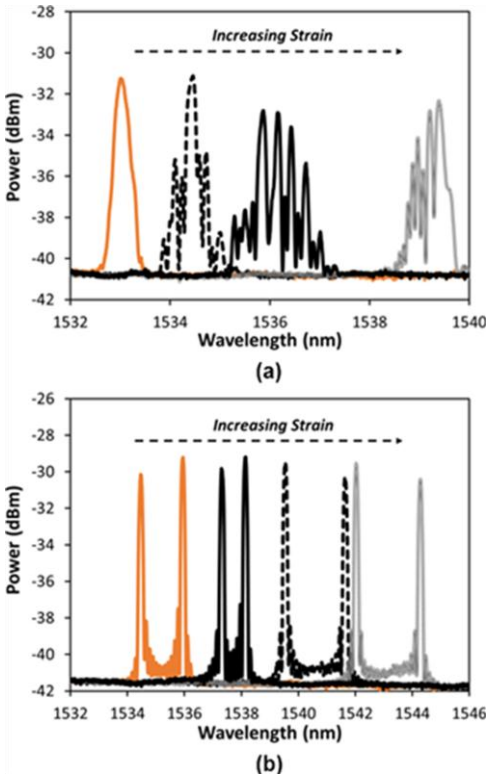

Figure 3. FBG wavelength shift and spectral distortion with increasing strain for a "medium" density parts.

The distorted fiber Bragg grating embedded in the medium density test specimen shifted to longer wavelengths with an increase in strain, as expected. The FBGs in both specimens shifted to longer wavelengths with increasing strain, as shown in Figure 3. It is theorized that non-uniform stresses due to torsion, compression, and tension was imparted on the FBG due to the greater spacing between the bond points on the fiber. The FBG spectra became progressively more distorted with an increase in strain and the FBG peak position could not be identified with the commercially available software. Thus, automated strain sensing of these parts could be not be performed with readily available technologies.

3.2. Embedded and Isolated FBGs

In an effort to reduce and/or eliminate the observed spectral distortion, a fiber Bragg grating was encased in fused quartz capillary tube prior to embedment into the plastic prototype part, as shown in Figure 4 (a). First, the acrylate coating was removed mechanically, thermally, and/or chemically, to expose the bare fiber. The fused quartz glass capillary was then "slid" over the bare fiber and positioned over the section of the fiber with the Bragg grating. Bare fiber must be exposed on both sides of the tube to allow for direct bonding between the extruded plastic and fiber surface. Otherwise, the plastic will bond to the acrylate coating, and upon tensile loading, the glass fiber may de-bond from the acrylate coating and slide within the coating. Subsequently, the tensile strain will not be transfer to the FBG. As shown in Figure 4 (b), no significant distortions were noticeable in the spectrum of the FBG embedded in the 3D printed prototype. The shift in position of the FBG to a lower wavelength was most likely attributed to minor residual strains in the optical fiber that evolved during the 3D printing process.

The FBG peak wavelength was readily monitored with the commercial peak tracking software upon tensile load of the 3D printed prototype, as shown in Figure 5. The glass capillary tube isolated the FBG from local and non-uniform strains and dramatically improved FBG peak wavelength fidelity. The strain sensitivity of the FBG was approximately

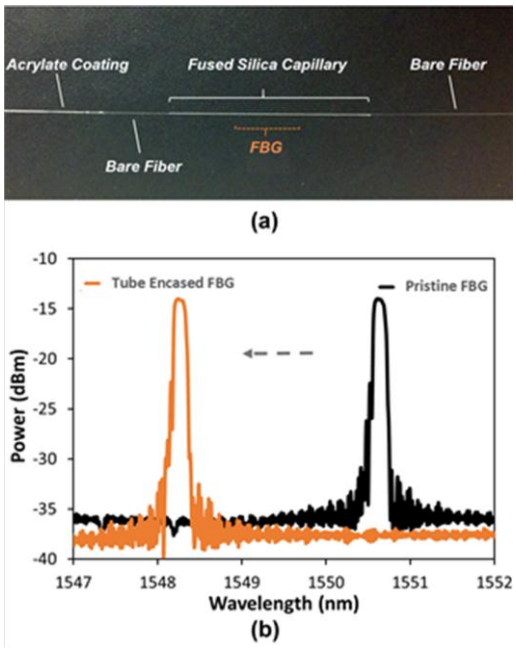

Figure 4. Peak wavelength shift of both FBG peaks upon stress loading and unloading. The difference between the two peak positions as a function of applied stress shown in the insert.

0.735 pm/kPa. Although the fiber broke at a tensile stress of approximately 8400 kPa, it is anticipated that further improvements to encapsulating and embedment procedures will improve the mechanical reliability of the sensing component.

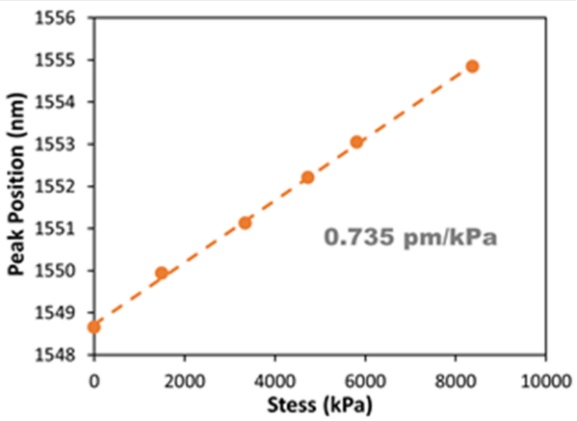

Figure 5. (a) Fused quartz capillary tube encased FBG configuration. (b) Spectral variations in tube encapsulated FBG embedded in a 3D printed PLA prototype.

4. CONCLUSIONS

Fiber Bragg grating sensors were successfully embedded into polymer parts via 3D printing. Distortions of the FBG spectra were observed due residual stresses in the fabricated components that were imparted on the fiber. Furthermore, wavelength hopping phenomena occurred in parts printed with higher densities. Spectral integrity was maintained for FBGs encased in a fused quartz capillary and peak wavelengths were readily distinguishable and monitored. Subsequently, the FBGs shifted to longer wavelengths upon tensile loading of the 3D printed test specimens. In situ embedding of FBGs was shown to be a feasible approach for real-time structural and component health monitoring.

ACKNOWLEDGEMENTS

The authors acknowledge Dr. Carlos Suchicital and Hesham Elmkharram for their assistance with the mechanical testing performed in this study.

REFERENCES

1. Carter PW, Advances in rapid prototyping and rapid manufacturing, Proceedings of Electrical Insulation Conference and Electrical Manufacturing & Coil Winding Conference, IEEE (2001) pp. 107-114.
2. Mironov V, Boland T, Trusk T, Forgacs G, Markwald RR, Trends Biotechnol. 21 (2003) 157.
3. Bak D, Assembly Autom. 23 (2003) 340.
4. Shashkov MM, Hess-Flores M, Recker S, Joy KI, owards Sensor-Aided Multi-View Reconstruction for High Accuracy Applications, CONTENT 2014, The Sixth International Conference on Creative Content Technologies (2014) pp. 65-69.
5. Rengier F, Mehndiratta A, von Tengg-Kobligk H, Zechmann CM, Unterhinninghofen R, Kauczor H-U, et al., Int. J. Comput. Assist. Radiol. Surg. 5 (2010) 335.
6. De Baere D, Strantza M, Hinderdael M, Devesse W, Guillaume P, Effective Structural Health Monitoring with Additive Manufacturing, EWSHM-7th European Workshop on Structural Health Monitoring (2014).
7. Alemohammad H, Toyserkani E., J. Manuf. Sci. Eng. 133 (2011) 031015.
8. Tu Y, Qi Y-H, Tu S-T., Smart Mater. Struct. 22 (2013) 075026.
9. Guo H, Xiao G, Mrad N, Yao J., Sensors 11 (2011) 3687.
10. Méndez A, Csipkes A, Overview of fiber optic sensors for NDT applications, In: Oğuz Güneş, Yılmaz Akkaya (Eds.), Nondestructive Testing of Materials and Structures, Springer, Springer (2013) pp. 179-84.
11. Pei H-F, Teng J, Yin J-H, Chen R, Measurement 58 (2014) 207.
12. Wong RY, Chehura E, James SW, Tatam RP, A chirped long period grating sensor for monitoring flow direction and cure of a resin, Proc. SPIE 8693, Smart Sensor Phenomena, Technology, Networks, and Systems Integration 2013, San Diego, California, USA (2013) p. 86930E.
13. Nielsen MW, Schmidt JW, Hattel JH, Andersen TL, Markussen CM., Wind Energy 16 (2013) 1241.
14. Chen F, Jiang Y., Meas. Sci. Technol. 25 (2014) 085106.
15. Kim S-W, Jeong M-S, Lee I, Kim E-H, Kwon I-B, Hwang T-K., Compos. Sci. Technol. 78 (2013) 48.
16. Kahandawa GC, Epaarachchi J, Wang H, Lau KT., Photonic Sens. 2 (2012) 203.
17. Jentoft LP, Dollar AM, Wagner CR, Howe RD., Sensors 14 (2014) 3861.
18. Kantaros A, Giannatsis J, Karalekas D, A novel strategy for the incorporation of optical sensors in Fused Deposition Modeling parts, Proceedings of Advanced Manufacturing Engineering and Technologies NEWTECH 2013,, Stockholm, Sweden (2013) p. 163.
19. Maier R, Havermanna D, Schnellera O, Mathewa J, Polyzosa D, MacPhersona W, et al., Optical Fibre Sensing in Metals by Embedment in 3D Printed Metallic Structures, Proc. of SPIE (2014) p. 915707.
20. Kantaros A, Karalekas D, In-situ monitoring of strain build up and temperature in a 3D polymer printing process, 16th International Conference on Experimental Mechanics (ICEM16) (2014) pp. 7-11.
21. Kantaros A, Karalekas D, Mater. Design 50 (2013) 44.
22. Kantaros A, Karalekas D, FBG Based In Situ Characterization of Residual Strains in FDM Process, SEM Annual Conference & Exposition on Experimental & Applied Mechanics,, Lombard, IL, USA (2013) p. 333.
23. Hill KO, Meltz G., J. Lightwave Technol. 15 (1997) 1263.
24.
25. Park C, Peters K., Meas. Sci. Technol. 23 (2012) 025105.
26. Prabhugoud M, Peters K., Smart Mater. Struct. 15 (2006) 550.
27. Ugale SP, Mishra V., Optik 125 (2014) 3822.
28. Zhou Z, Li J, Ou J., Front. Electr. Electron. Eng. Chin. 2 (2007) 92.
29. Ling H-Y, Lau K-T, Jin W, Chan K-C., Opt. Commun. 270 (2007) 25.
30. Rodriguez-Cobo L, Cobo A, Lopez-Higuera J-M., Composites Part B 53 (2013) 284.
31. Webb S, Peters K, Zikry M, Vella T, Chadderdon S, Selfridge R, et al., Meas. Sci. Technol. 22 (2011) 065301.
32. Abrishamian F, Nakai Y, Sato S, Imai M., Opt. Fiber Technol. 13 (2007) 32.
33. Fangdong Zhu FZ, Dongsheng Zhang DZ, Peng Fan PF, Litong Li LL, Yongxing Guo sYG., Chin. Opt. Lett. 11 (2013) 100603.
34. Majumder M, Gangopadhyay TK, Chakraborty AK, Dasgupta K, Bhattacharya DK, Sens. Actuat. A 147 (2008) 150.
35. Liu W-F, Liu I, Chung L-W, Huang D-W, Yang C., Opt. Lett. 25 (2000) 1319.

Cite this article as:

Daniel Homa *et al.*: Fiber Bragg gratings embedded in 3D printed prototypes. Sci. Adv. Today 2 (2016) 25242.